

Learning Concise and Descriptive Attributes for Visual Recognition

An Yan^{*◇}, Yu Wang^{*◇}, Yiwu Zhong^{*♣}, Chengyu Dong[◇], Zexue He[◇],
 Yujie Lu[♣], William Yang Wang[♣], Jingbo Shang[◇], Julian McAuley[◇]
[◇]UC San Diego, [♣]University of Wisconsin-Madison, [♠]UC Santa Barbara
 {ayan, yuw164, cdong, zehe, jshang, jmcauley}@ucsd.edu
 {yujielu, william}@cs.ucsb.edu, yzhong52@wisc.edu

Abstract

Recent advances in foundation models present new opportunities for interpretable visual recognition – one can first query Large Language Models (LLMs) to obtain a set of attributes that describe each class, then apply vision-language models to classify images via these attributes. Pioneering work shows that querying thousands of attributes can achieve performance competitive with image features. However, our further investigation on 8 datasets reveals that LLM-generated attributes in a large quantity perform almost the same as random words. This surprising finding suggests that significant noise may be present in these attributes. We hypothesize that there exist subsets of attributes that can maintain the classification performance with much smaller sizes, and propose a novel learning-to-search method to discover those concise sets of attributes. As a result, on the CUB dataset, our method achieves performance close to that of massive LLM-generated attributes (e.g., 10k attributes for CUB), yet using only 32 attributes in total to distinguish 200 bird species. Furthermore, our new paradigm demonstrates several additional benefits: higher interpretability and interactivity for humans, and the ability to summarize knowledge for a recognition task.

1. Introduction

Explaining black-box neural models is a critical research problem. For visual recognition, one line of research tries to classify objects with descriptions or attributes [12, 8, 39, 18, 22], which provide additional information beyond visual cues such as activation maps [41, 40]. However, they require in-depth human analysis and intensive annotation to obtain key attributes for a particular recognition task. Such a paradigm is costly and thus impractical to scale up when the number of classes and domains grows.

The recent advance of language foundation models cre-

* equal contributions.

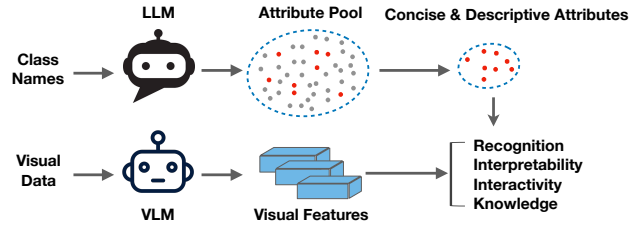


Figure 1: Our proposed paradigm for visual recognition via learning a concise set of descriptive attributes.

ates new opportunities for building interpretable visual recognition models, as demonstrated by the powerful capabilities of models such as GPT-3 and ChatGPT in encoding world knowledge [5, 32, 21]. One can query useful visual attributes from LLMs and classify images via these attributes by converting visual features from vision-language models (VLMs) (e.g., CLIP [36]) into attribute scores [56]. One recent work [52] shows that a large set of attributes from LLMs (e.g., 50 attributes per class) can achieve comparable performance to image features in a linear probing setting. However, two key observations motivate us to rethink this formulation: (1) A large number of attributes dramatically hurts the interpretability of a model. It is unrealistic to manually check thousands of attributes to fully understand model decisions. (2) We surprisingly find that when the number of attributes is large enough (e.g., the dimension of image features), random words drawn from the entire vocabulary can perform equally well as LLM-generated attributes. Moreover, reducing the number of random words by 25% can still attain competitive performance. This indicates that redundant and noisy information exists in the massive LLM-generated attributes.

With our findings, we ask the research question: *Can we learn a concise set of representative visual attributes in the form of natural language to explain how visual recognition works?* **For example, can we find a few representative attributes to distinguish 200 bird species?** This is a non-trivial problem. Even for humans, it is not easy to summa-

size what are the representative visual attributes given many visual classes. To tackle this challenge, we propose a novel learning-to-search method, which uses image-level labels to guide the searching of discriminative attributes. Specifically, we train a learnable dictionary to approximate the embedding space of VLMs, and then find descriptive attributes in the latent text space via nearest neighbor search.

In summary, we propose a new paradigm for visual recognition (Figure 1), which seeks to learn a concise set of visual attributes in the form of natural language. Once learned, there are several benefits to our new paradigm: **(1)** Our discovered attributes are highly descriptive. On 8 visual recognition datasets, our model classifies images via these attributes and achieves comparable classification performance as image features, even if the number of attributes is much smaller than the dimension of image features. **(2)** The condensed sets of attributes enable strong interpretability for the model decision process through a few human-friendly text descriptions. **(3)** Additionally, our framework presents a natural language interface for humans to interact with. One can correct a wrong prediction during model inference, by perturbing the values of attribute scores where it made mistakes. **(4)** Lastly, these expressive attributes can be viewed as a concise form of knowledge to summarize useful features for a visual recognition task, without costly human effort.

Overall, our contributions are three-fold:

- Leveraging recent advances in foundation models, we propose a new paradigm for visual recognition by learning a concise set of attribute descriptions.
- To find these attributes, we propose a novel learning-to-search method which prunes the large attribute pool from large language models to a descriptive subset.
- We conduct extensive experiments across 8 visual recognition datasets to validate our recognition effectiveness and efficiency with additional benefits.

2. Methodology

In this section, we introduce our key components for a new paradigm of visual recognition. It mainly consists of three modules: **First**, in Section 2.1, given an image domain, we query large language models to obtain a large set of visual attributes for the categories of a task. **Second**, we use a semantic transformation (Section 2.2) to project the image features into attribute features via a vision-language model, where each dimension in the new space corresponds to an attribute concept, and a higher value represents higher correlation between the image and the attribute. **Finally**, given the large space of attributes, we propose a novel learning-to-search method (Section 2.4) to efficiently prune the attributes into a much smaller subset to obtain a concise model for classification.

2.1. Generating Attribute Concepts via LLMs

The first step of our framework is to obtain a set of appropriate attribute concepts. Given a dataset with different categories, (e.g., CUB with 200 bird classes), what are the distinctive visual attributes to recognize them? Manually labeling and designing these attribute concepts can be costly, and can not scale to large numbers of classes. Large Language Models (LLMs), such as GPT-3 [5] and ChatGPT, provide an alternative solution. We can view these language models as implicit knowledge bases with exceptional world knowledge on a variety of tasks and topics, which humans can easily interact with through natural language to query knowledge. To this end, prompt engineering, or the ability to ask good questions to language models, is still important. To effectively query knowledge from LLMs with regard to classifying images, we design two types of prompts.

Instance Prompting for Class-level Features. For each class c in a given task, our first design choice is to query class-level information from LLMs. We prompt a language model with the instance prompt:

Q: What are the useful visual features to distinguish Y_c in a photo?

where Y_c corresponds to the name of class c in the form of natural language.

Batch Prompting for Group-level Features. For certain datasets (e.g., CIFAR-100 and ImageNet), there is inherently a hierarchy that some categories belong to the same group. For example, in CIFAR-100, there is a superclass for every five categories. Hence, we propose batch prompting, where we ask the language model to reason about the distinctive visual features among a batch of categories:

Q: Here are N_g kinds of Y_g : $\{Y_{c_1}, Y_{c_2}, \dots, Y_{c_M}\}$. What are the useful visual features to distinguish them in a photo?

where N_g is the number of classes in a group g , Y_g is the name of the group, Y_{c_i} corresponds to the name of each class c_i in the form of natural language.

We present more details regarding our prompt design, robustness check of different prompts, and examples of the generated attributes in Appendix A.

2.2. Semantic Projection

After obtaining a pool consisting of N attribute concepts $\mathcal{C} = \{a_1, a_2, \dots, a_N\}$, the second challenge is how we can best leverage these attributes to build interpretable image classifiers. Recent advances of vision-language models such as CLIP bridge the gap between images and text, by pre-training models with large scale image-text pairs. Intuitively, converting from images to text is a discretization process that will unavoidably lose rich semantic information stored in an image.

To better preserve information, we use a semantic projection that transforms a visual feature into an attribute

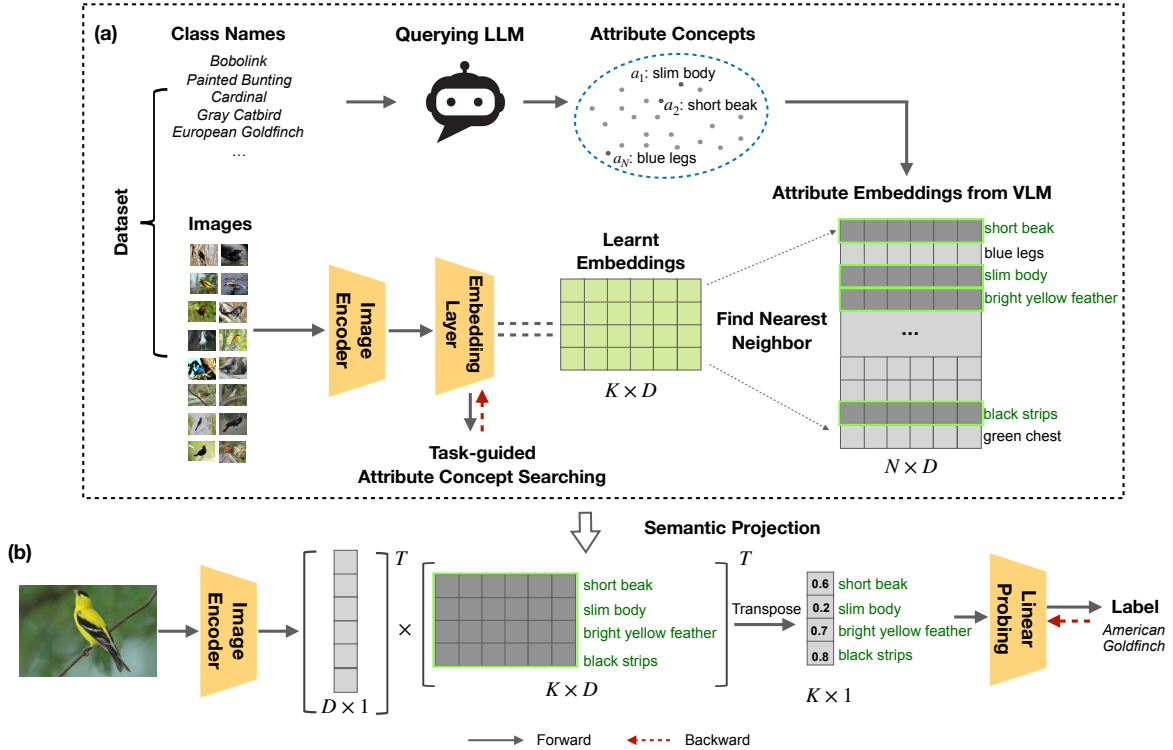


Figure 2: The framework of our model. (a) Querying attributes from LLMs and finding a concise set of representative attributes; (b) An example using the attributes for interpretable visual recognition.

concept space. Given an image I , we convert the D -dimensional image feature $\mathbf{V} \in \mathbb{R}^D$ into an N -dimensional attribute concept vector $\mathbf{A} \in \mathbb{R}^N$:

$$\begin{aligned} \mathbf{V} &= \Theta_V(I), \mathbf{T}_i = \Theta_T(a_i) \\ s_i &= \cos(\mathbf{V}, \mathbf{T}_i), i = 1, \dots, N \\ \mathbf{A} &= (s_1, \dots, s_N)^T \end{aligned} \quad (1)$$

where $\cos(\cdot, \cdot)$ is the cosine similarity between two vectors, s_i is the cosine similarity between two vectors. Θ_V and Θ_T are the visual and text encoder of a VLM. \mathbf{T}_i is the embedding of the i -th attribute in the attribute concept pool, $i \in \{1, \dots, N\}$. \mathbf{A} is the semantic vector of image I .

2.3. The Hypothesis of Attribute Concept Space

Conceptually, our semantic projection resembles principal component analysis, where we aim to find a set of bases in the form of natural language, and by projecting the images into these bases we obtain a new attribute concept space where each dimension in the space corresponds to a visual attribute concept. However, the large bag of attribute concepts we obtained from large language models is not the optimal language basis. As of today, LLMs are models that noisily condense world knowledge from the web,

and are not optimized for visual recognition or visual reasoning tasks. We hypothesize that there exist subsets of attributes that can still achieve high classification performance with a much smaller size. Intuitively, most attributes in the large attribute concept pool are irrelevant to classify a certain class. For example, attributes that describe dogs are less likely to be suitable attributes to recognize birds or cars. Practically, formatting a compact attribute set is also helpful for humans to interact with the model and understand its behavior better. A small number of attributes is much easier for diagnostic purposes and making decisions with these neural models, which is the ultimate goal of building interpretable models.

2.4. Task-Guided Attribute Concept Searching

Finding an expressive set of language bases is non-trivial. The massive attributes from LLMs are noisy, and finding a few representative attributes for hundreds of classes in a task can be challenging and costly, even for human experts with domain knowledge. An exhaustive search is also impractical given the large text space.

Inspired by dictionary learning and vector quantization techniques [43], we present a learning-to-search method that learns a dictionary to approximate an expressive sub-

set of attributes given fixed K . Specifically, we first define an embedding matrix $\mathbf{E} \in \mathbb{R}^{K \times D}$, where K is a K -way categorical that equals the number of attributes, and D is the dimensionality of embedding vectors \mathbf{V} and \mathbf{T}_i (*i.e.*, the latent dimension of VLMs), where \mathbf{V} and \mathbf{T}_i is the image embedding and the i -th attribute embedding shown in Eq.(1). Since our goal is to find K attributes to be expressive, we propose a task-guided attribute concept searching method to optimize for a particular task. For visual recognition tasks, we use a classification head to project the dictionary into K_C classes and guide the learning process with the categorical cross-entropy loss:

$$\mathcal{L}_{ce} = -\frac{1}{M} \sum_{i=1}^M \sum_{c=1}^{K_C} y_{i,c} \log(p_{i,c}) \quad (2)$$

where M is the number of images in a mini-batch, $y_{i,c}$ is the binary indicator of the i -th image in the mini-batch belonging to class c , and $p_{i,c}$ is the predicted probability of the i -th image belonging to class c .

But simply training with the guidance of the cross-entropy loss is suboptimal, as the embeddings \mathbf{E} are not in the same space of \mathbf{T} . Thus, we use the Mahalanobis distance as a constraint to encourage the embeddings to be optimized towards the latent space of vision-language models. Given a sampled probability distribution \mathbf{T} , the Mahalanobis distance of \mathbf{E}_j from \mathbf{T} is defined as

$$\mathcal{D}_{mah}^j = \sqrt{(\mathbf{E}_j - \boldsymbol{\mu})\mathbf{S}^{-1}(\mathbf{E}_j - \boldsymbol{\mu})} \quad (3)$$

where $\boldsymbol{\mu} = (\mu_1, \dots, \mu_D)$ is the mean vector and \mathbf{S} is the positive-definite covariance matrix of \mathbf{T} . Then the regularization term is defined as:

$$\mathcal{L}_{mah}^j = \frac{1}{K} \sum_{j=1}^k \mathcal{D}_{mah}^j \quad (4)$$

Overall, our model is optimized with a mixture of two losses:

$$\mathcal{L}_{loss} = \mathcal{L}_{ce} + \lambda \sum_{j=1}^K \mathcal{L}_{mah}^j. \quad (5)$$

After training, we have the embedding matrix \mathbf{E} which will be used for searching the attributes from the attribute concept pool \mathcal{C} . Note that for $\mathbf{E} \in \mathbb{R}^{K \times D}$, each row of \mathbf{E} is a D -dimensional vector. We denote the j -th row of \mathbf{E} as \mathbf{E}_j . We use greedy search as follows:

$$\begin{aligned} \mathbf{T}_j^* &= \arg \max_{i \in \{1, \dots, N\}} \cos(\mathbf{T}_i, \mathbf{E}_j), \\ \text{s.t. } \mathbf{T}_j^* &\neq \mathbf{T}_k^*, \forall 1 \leq k < j, \end{aligned} \quad (6)$$

where j is from 1 to K ,

As j iterates from 1 to K , we can find K attribute embeddings $\mathbf{T}_j^*, j \in \{1, \dots, K\}$, which corresponds to K expressive attribute concepts and are the condensed features containing the necessary knowledge for the task. With the selected attributes, we can calculate the semantic vector of each image as in Eq. (1), where each dimension of the vector is a similarity score between the image and an attribute. We evaluate the performance of these semantic vectors with linear probes, and the obtained linear model is used for inference and analysis.

3. Experiments

3.1. Experimental Setup

Datasets We conduct our experiments on 8 different image classification datasets, including: CUB [44], CIFAR-10 and CIFAR-100 [24], Food-101 [4], Flower [31], Oxford-pets [33], Stanford-cars [23], Imagenet [9]. For Imagenet, it is not trivial to analyze all 1000 diverse classes. So we narrow the scope to 397 animal classes, with 509,230/19,850 samples for train/test. We denote this subset as Imagenet-Animals. For other datasets, most of them include images within a specific domain (CUB, Flower, Food, Oxford-pets, Stanford-cars), while CIFAR-10 and CIFAR-100 contain broader classes that lie across domains.

Implementation Details Our method involves two stages of training. The first stage consists of task-guided learning of a dictionary \mathbf{E} to approximate CLIP text embeddings and using this dictionary to find K attributes for visual recognition. For the Mahalanobis distance, the parameter λ is tuned with a grid search in $\{1, 0.1, 0.01, 0.001, 0\}$. The second stage is one-layer linear probing to classify semantic vectors. The batchsize is set to 4,096 for all datasets except 32,768 on Imagenet-Animals for faster converging. We set the number of epochs to 5,000 epochs with early stopping. The learning rate is set to 0.01 in all experiments with an Adam optimizer [20]. Unless specified, we use GPT-3 and CLIP ViT-B/32 for all performance comparison.

Baselines We compare with state-of-the-art works that leverage attributes either from human annotations or from LLMs. For a fair comparison, we use linear probes to evaluate all methods: (1) **CompDL** [56] builds semantic vectors using CLIP scores between human-designed attributes and images. (2) **LaBO** [52] is a recent work that builds semantic vectors with a large set of attributes from LLMs. (3) **Human** [44, 22]. Attribute labels for each image are annotated by humans. We compare with two versions: binary labels for each attribute, and calibrated labels with confidence scores given by annotators.

To validate the effectiveness of learning-to-search, we explore other baselines: (1) **K-means**. Perform K-means

Datasets	CUB			CIFAR-10			CIFAR-100			Flower		
K	32	200	400	8	10	20	64	100	200	32	102	204
LaBo	–	60.93	62.61	–	78.11	84.84	–	75.10	76.94	–	80.98	86.76
Ours	60.27	63.88	64.05	77.47	80.09	87.99	73.31	75.12	77.29	80.88	87.26	89.02
Datasets	Food			Oxford_Pets			Stanford_cars			Imagenet_Animals		
K	64	101	202	16	37	74	64	196	392	128	397	794
LaBo	–	79.95	81.33	–	76.91	84.33	–	72.33	74.39	–	74.88	75.49
Ours	78.41	80.22	81.85	76.29	83.15	85.91	72.07	74.57	75.56	74.48	75.69	75.83

Table 1: Comparison with state-of-the-art. LaBo is designed to use at least as many attributes as classes. We use “–” to denote non-applicability.

K (# of attributes)	8	16	32	312
Human Binary [44]	4.02	7.31	10.11	47.38
Human Calibration [22]	3.75	7.15	9.78	43.37
CompDL [56]	12.64	26.41	28.69	52.60
Ours	31.67	48.55	60.27	65.17

Table 2: Comparison with human annotations on CUB.

clustering on CLIP attribute embeddings, then find K attributes with nearest distance to each clustering center. Intuitively this can be a strong baseline, as K attributes close to each center can be distinctive. (2) **Uniform Sampling** from the large attribute pool. (3) **SVD**. After obtaining the attribute embeddings \mathbf{T} , we run SVD decomposition of \mathbf{T} to get the top K vectors and find attributes with the largest similarity with the K important vectors. (4) **Similarity**. We calculate the average score of each attribute across all images and then find the K attributes with the largest average scores. (5) **Img Features**. Black-box linear probing on latent image features with two linear layers and an intermediate dimension K as a reference.

3.2. Main Results

Comparison with previous work We first compare our method with LaBo [52]. It is designed to use M_c concepts per class with default number of 50, which corresponds to 10,000 attributes for CUB. For fair-comparison, we set M_c as 1 and 2 in the experiments. As shown in Table 1, our method outperforms LaBo with the same number of attributes on both the full and few-shot setting. Furthermore, our method can achieve similar accuracy with only a smaller number of attributes (e.g., 32 attributes for CUB). These results suggest that our learned attributes are discriminative enough to classify the images, despite given much fewer attributes.

We then further compare with human annotations from CUB. For $K < 312$, we select attributes based on their

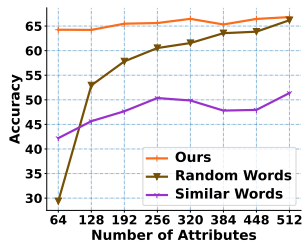


Figure 3: Performance comparison with random or similar words on CUB.

	Examples
R	boy champagne allied whose acrobat eight centered lobby heads
S	red,gray,snow wings orange wings lime,navy wings
G	sloping forehead distinctive white throat bright red head and breast

Table 3: Examples from Random (R), Silimilar (S), GPT-3 (G) attributes

accumulated confidence score for all samples. As shown in Table 2, human annotated attributes are more noisy than CLIP similarities. With the same attributes, CLIP scores from CompDL build more expressive features. Furthermore, our LLM-suggested attributes significantly outperform human designs, e.g. by using 16 attributes we achieve similar performance as 312 attributes defined by humans.

Large-scale attributes behave like random words We present our finding that LLM-generated attributes in a large quantity behave like random words. Specifically, we compare our method of using GPT-3 attributes with random or similar words. Here, we constructed random words by randomly choosing 1-5 words from the entire English vocabulary, and semantically similar words by combining 1-3 random colors with the noun “wings” as suffix. As shown in Figure 3, when $K = 512$, random words perform as well as GPT-3 attributes in terms of classification accuracy. Even reducing K from 512 to 256 does not significantly hurt its performance. But when K is small (e.g., 64), the performance of random words drops dramatically. We conjecture that it is because text embeddings randomly drawn from CLIP are nearly orthogonal bases [45]. Given an image feature $\in \mathbb{R}^D$, projection with a set of $K=D$ orthogonal bases can perfectly preserve its information. We further

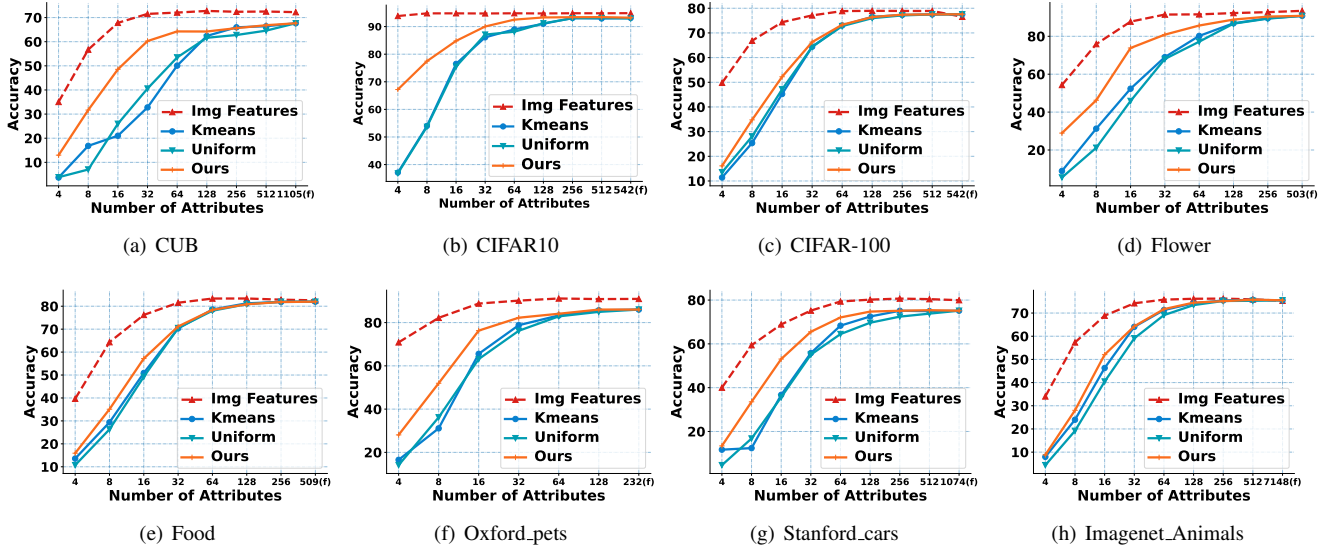


Figure 4: Overall Performance on all datasets. X-axis: number of attributes, Y-axis: Accuracy (%), “(f)” means “full”, *i.e.*, all attributes in the pool are used. Uniform refers to uniform sampling.

explore how similar words (e.g., red wings, yellow wings) behave. Embeddings of similar words in a trained language model are not orthogonal bases hence the projection will lose information when K is large (e.g., intuitively it is hard to classify 200 bird species using only the color combination of wings). But as K gets smaller, since those similar words have close semantic meanings, they start to outperform random words. Overall, these findings motivate us to find a concise set of meaningful attributes while maintaining competitive performance.

Number of attributes and selection methods Finally, we study performance change under different number of attributes in Figure 4. First, our method is competitive with image features when K is large. Reducing number of attributes K to the number of classes C (e.g., 512 to 128 for CUB) does not significantly hurt performance, even for baseline methods. This validates our hypothesis that there is plenty of redundant information in the semantic space when the number of attributes is large (as used in LaBO [52]). It is possible to find a subset of expressive attributes for visual recognition. Second, we also consistently outperform other methods such as K-means clustering and uniform sampling, demonstrating the effectiveness of our task-guided searching method. Third, a heuristic design such as K-means performs similar as uniform selection. Note that though there is a performance gap between image features and using attributes, the gap can be minimized by using a stronger VLM, as the classification accuracy of attributes relies on the accurate estimation of the correlation between images and attributes (see more results in appendix D).

Datasets	CUB			CIFAR-100		
	K	8	16	32	8	16
GPT-3	31.67	48.55	60.27	34.77	52.24	66.30
GPT-3-Imagenet	30.81	49.29	60.41	33.80	51.01	65.61

Table 4: Ablation study *w.r.t.* different concept pools.

3.3. Ablation Study

Robustness to the attribute pool First, we aim to explore the effects of different initialized attribute concept pools generated by LLMs. On CUB and CIFAR-100, we compare two attribute pools, attributes generated from classes in each dataset, and attributes generated from the full set of ImageNet classes. As shown in Table 4, even with the large and noisy attributes from ImageNet, our method can still efficiently find a small number of representative attributes for a task, and obtains competitive classification performance.

Effectiveness of learning-to-search Then, we discuss possible choices for selection out of the large attribute pool. Results are shown in Table 5 with the following observations: heuristic methods such as K-means and SVD are not optimal choices for identifying the most distinctive attributes. In fact, they are sometimes less effective than uniform sampling. This is likely because we need to identify the most distinguishing attributes for visual recognition, rather than the most diverse ones based on text embeddings. Overall, our method significantly outperforms other baseline selection methods, showing its efficacy.

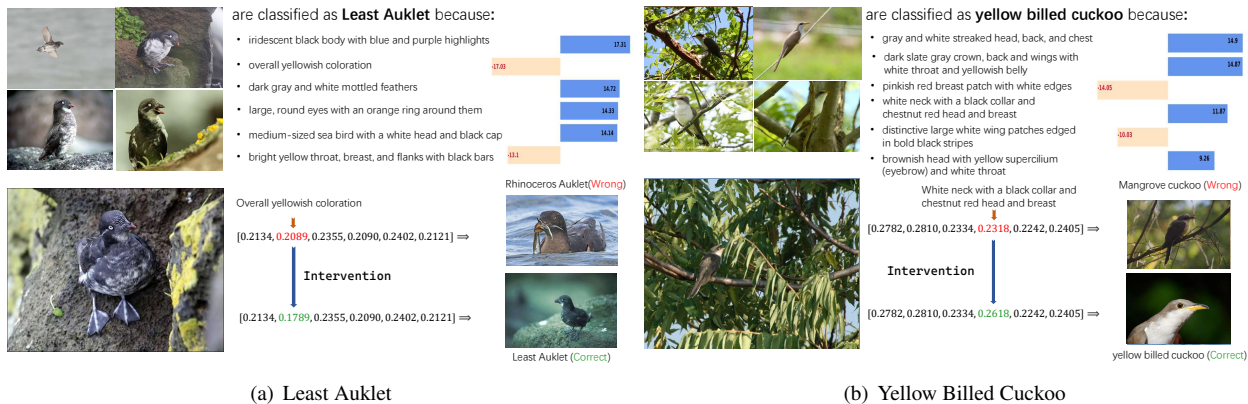


Figure 5: Examples on interpretability and interactivity. (1) The upper half of each figure show important attributes for two classes of birds. We choose 6 out of 32 attributes with highest importance scores, which are computed by multiplication between clip scores and weights in the linear probe, defined in Eq. (7). (2) The lower half of each figure demonstrates the intervention on the semantic vector (i.e., CLIP scores) to correct the prediction, we use $\delta=0.03$ for all interventions on clip scores as an empirical value. The array of 6 scores are of the same order as the attributes.

Datasets	CUB			CIFAR-100			
	K	8	16	32	8	16	32
K-means		16.83	21.02	32.76	25.39	45.26	64.41
Uniform		7.02	25.98	40.58	28.07	47.14	64.34
SVD		6.52	20.02	35.83	29.06	50.00	64.99
Similarity		4.73	9.72	18.00	26.75	45.61	62.79
Ours		31.67	48.55	60.27	34.77	52.24	66.30

Table 5: Ablation study *w.r.t.* different attribute selection strategies.

Dataset	CUB				
	K	8	16	32	64
MAH		30.76	47.87	60.27	64.25
COS		28.96	47.35	58.27	63.25
CE		31.67	48.55	55.88	60.73
Dataset	CIFAR-100				
	K	8	16	32	64
MAH		34.77	52.24	65.91	73.31
COS		31.98	51.15	65.02	72.80
CE		32.45	50.83	66.29	73.25

Table 6: Ablation study *w.r.t.* different regularization.

Effectiveness of regularization We compare the Mahalanobis distance (MAH) with two variations: (1) COS: For each vector \mathbf{E}_j and \mathbf{T}_i (of the i -th attribute) in the concept pool, we computed averaged cosine distance as follows:

$$\mathcal{L}_{cos} = \frac{1}{K^2} \sum_{j=1}^K \sum_{i=1}^K \frac{\mathbf{T}_i^\top \mathbf{E}_j}{\|\mathbf{T}_i\| \|\mathbf{E}_j\|}$$

(2) CE: Learning with Eq. (2) only. Results are in Table 6. Overall, Mahalanobis distance is an effective constraint to encourage the dictionary E to be close to the distribution of CLIP embeddings.

3.4. Analysis of Interpretability and Interactivity

We perform analysis and visualizations to show that:

(1) **Our learned attributes provide interpretability.** As shown in Figure 5, the upper half presents the images in a class c and high relevant attributes to recognize them. Specifically, we denote $\mathbf{W} \in \mathbb{R}^{K_C * K}$ as the weight of the

FC layer in linear probing, where K_C , K are the number of classes and attributes. Then for each image i and its semantic vector $\mathbf{A} \in \mathbb{R}^K$, we multiply the corresponding score vector of image i with the corresponding row of the FC layer \mathbf{W}_c to compute Importance Score $\mathbf{IS} \in \mathbb{R}^K$:

$$\mathbf{IS} = \mathbf{W}_c \otimes \mathbf{A} \quad (7)$$

where \otimes means element-wise multiplication. Then we present attributes with the top absolute values of \mathbf{IS} averaged over all samples in a class from the test set, with blue/orange bars indicating the positive/negative importance. Higher absolute values denote greater significance. Since all CLIP scores are positive [16], the positivity or negativity of high IS signifies their relevance to the class.

(2) **Our concise set of attributes enables simple interactivity.** As shown in the lower half of Figure 5, we can correct the model’s wrong predictions during inference by changing only a single similarity score between an image


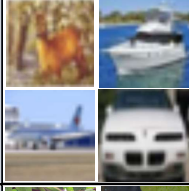

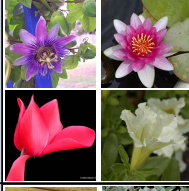

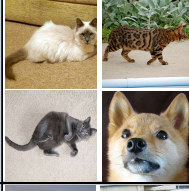
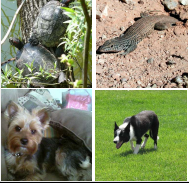
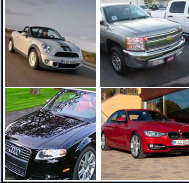
CUB		<ul style="list-style-type: none"> • distinctive white throat • bright red head and breast • pinkish red breast patch with white edges • bright yellow, green and blue plumage • Red face with a black cap and bib • Short legs for perching on reeds • white and black spotted breast • sloping forehead 	CIFAR10		<ul style="list-style-type: none"> • antlers (in males) • pointed bow and stern • propellers or jet engines • moist slimy skin • long head with a mane and tail • landing gear • portholes along the hull • four wheels
CIFAR100		<ul style="list-style-type: none"> • a seat for the rider • catkins (flowers) in spring • many windows in the façade • five pairs of walking legs • smooth oval shaped sepals • four-limbed primate • headboard and footboard • towers with conical roofs 	Flower		<ul style="list-style-type: none"> • Shiny wax coating on the spathe • large, yellow or orange flower head • bright pink color • large, white petals with a yellow center • pink to purple colored petals with red lips • bright red and yellow petals • pink, white, or lavender flowers with five petals • deep purple or blue flowers
Food		<ul style="list-style-type: none"> • elbow macaroni noodles • Shredded pork meat in the middle of the sandwich • large pieces of clams visible in the chowder • usually served in a warm wrap or burrito shell • sliced into thin wedges or cubes • thinly sliced raw fish • tender squid rings inside • a crisp, fried pastry dough exterior 	Oxford Pets		<ul style="list-style-type: none"> • black and tan coloring • short coat of glossy black fur • Long legs and neck • Shade of red or wheaten color • large, round eyes • Pointed ears • white blaze on face and chest • greyish blue fur with silver tips
Imagenet Animals		<ul style="list-style-type: none"> • male finches have a bright red breast • brownish-yellow fur • small, four-limbed canid • long, black, shiny body • the carapace is rough and bumpy • white spots on the crab's shell • English setters are bred in England • long, wirehaired coat 	Stanford Cars		<ul style="list-style-type: none"> • signature Lincoln split headlamps • large front grille with the signature BMW kidney shape • large size with a wheelbase of 149.4 inches • "4Runner" badge on the rear liftgate • signature SRT8 grille with crosshair pattern • Porsche logo on front grille and trunk lid • S6 badge on the trunk lid • unique HUMMER H2 logo on front grille

Figure 6: A concise set of 8 descriptive attributes learned for each dataset with sampled images.

and the attribute that the CLIP model made a mistake on. This is a significant simplification compared with previous work [22] where they need to manipulate scores from a group of concepts for the CUB dataset. We present more user studies in appendix E.

3.5. Visualization of Our Discovered Attributes

We show our learned descriptive attributes with $K = 8$ in Figure 6. Intuitively, we can observe these attributes are distinctive for each domain. Take birds recognition (CUB) as an example, the eight attributes covered most of the body parts of a bird (head, breast, legs, etc.). As we are condensing knowledge from hundreds of bird classes, each attribute broadly covers many categories. A bright red head and breast can be a noticeable visual attribute for many bird species, such as the Northern Cardinal and the Vermilion Flycatcher. Overall, explaining a domain with a few descriptive attributes is challenging, even for an expert with sufficient domain knowledge. But our model is able to automatically provide a level of knowledge to help humans understand how visual recognition works.

We then present case studies on CIFAR-10 with 4 attributes and CLIP scores of 10 random images from each class in Figure 7. In general, each image is activated in a distinguishable way in the heat map. Some attributes can distinguish a few classes, for example, cat and dog have



Figure 7: Case study on CIFAR-10. The numbers are CLIP similarity scores between each image and attributes.

higher activation on “fur coat” compared to automobile or truck. Thus “fur coat” may be an important feature to differentiate animals and vehicles.

4. Related work

Interpretable Deep Learning Interpretability is a critical research problem for deep learning with black-box models [11, 34, 37, 38, 13, 2, 50]. Some works study model behavior and explore if deep models could encode concepts for understanding [19, 28, 49, 29]. For image classification, preliminary attempts aim to describe objects with attributes [12, 26, 25] or building concept bottleneck mod-

els [22, 56, 55, 6]. These methods require in-depth human analysis and intensive labeling, which are impractical to scale to more classes and domains.

Recent works [30, 35, 52] tackle this problem by using GPT-3 as a knowledge base to query visual attributes or concepts. Specifically, [30, 35] generate descriptions with LLMs, and use them for knowledge-aware prompting for each class to improve zero-shot performance of CLIP [36]. For example, given the class name “bee”, it will augment it with attributes such as “A bee with black and yellow body”. Our work differs in that our goal is to learn representative attributes for visual recognition without using class names. LABO [52] extends the idea of concept bottleneck models by generating thousands of concepts from LLMs. Inspired by our finding that there is great redundancy in the large-scale attributes, we aim to learn a concise set of attributes that are initially generated from LLMs for each task, while maintaining the classification performance as possible. Concise attributes also enable stronger interpretability and interactivity, and can help humans to summarize critical knowledge for visual recognition in an automatic way.

Foundation Models Recently, foundation models [3], which are pre-trained with a large amount of data and large model sizes, have revolutionized machine learning research and many fields. These models are shown to be adaptable to a wide range of downstream tasks for computer vision [15, 46, 58], natural language processing [10, 7, 57, 48] and cross-modal research [27, 42, 17, 14]. One direction is to train LLMs such as GPT3 [5] and ChatGPT with massive text to serve as a powerful knowledge base with high interactivity and beyond. Another direction is to build VLMs [36, 51, 54, 53, 1], which connect vision and language by pre-training with image-text pairs and learning a joint embedding space for both. In this work, we use LLMs as a knowledge base for querying visual related knowledge, and use VLMs to bridge vision and text, presenting a new paradigm for interpretable visual recognition in the era of foundation models.

5. Discussion

There are many interesting topics to explore with our new paradigm. First, our framework is a plug-and-play model that can be readily applied to many other vision tasks, by simply changing the task-guided learning objective to a particular task, e.g., classification losses for object detection, video understanding, and 3D classification. Furthermore, a concise set of descriptive attributes enables interactivity for vision models and empowers human-machine cooperation in a user-friendly way through natural language interfaces. Lastly, we show the potential of summarizing knowledge for challenging vision tasks in the new era of LLMs, which could have broad impact for various domains.

6. Conclusion

In this work, we propose a new paradigm for visual recognition that leverages a concise set of descriptive attributes. Motivated by our insightful finding that significant redundancy exists in massive LLMs-generated attributes, we design a simple yet effective searching method guided by image-level labels, to identify an informative subset. Our new paradigm is validated across 8 datasets to achieve strong classification accuracy with multiple benefits and broad impacts, including efficiency, interpretability, human interactivity, and knowledge summarization.

Acknowledgments

We would like to sincerely thank the anonymous reviewers and chairs for their careful review of our work, with helpful and constructive suggestions to improve the paper.

References

- [1] Jean-Baptiste Alayrac, Jeff Donahue, Pauline Luc, Antoine Miech, Iain Barr, Yana Hasson, Karel Lenc, Arthur Mensch, Katie Millican, Malcolm Reynolds, et al. Flamingo: a visual language model for few-shot learning. *arXiv preprint arXiv:2204.14198*, 2022. 9
- [2] Alina Jade Barnett, Fides Regina Schwartz, Chaofan Tao, Chaofan Chen, Yinhao Ren, Joseph Y. Lo, and Cynthia Rudin. A case-based interpretable deep learning model for classification of mass lesions in digital mammography. *Nat. Mach. Intell.*, 3(12):1061–1070, 2021. 8
- [3] Rishi Bommasani, Drew A Hudson, Ehsan Adeli, Russ Altman, Simran Arora, Sydney von Arx, Michael S Bernstein, Jeannette Bohg, Antoine Bosselut, Emma Brunskill, et al. On the opportunities and risks of foundation models. *arXiv preprint arXiv:2108.07258*, 2021. 9
- [4] Lukas Bossard, Matthieu Guillaumin, and Luc Van Gool. Food-101 - mining discriminative components with random forests. In *ECCV (6)*, volume 8694 of *Lecture Notes in Computer Science*, pages 446–461. Springer, 2014. 4
- [5] Tom Brown, Benjamin Mann, Nick Ryder, Melanie Subbiah, Jared D Kaplan, Prafulla Dhariwal, Arvind Neelakantan, Pranav Shyam, Girish Sastry, Amanda Askell, et al. Language models are few-shot learners. *Advances in neural information processing systems*, 33:1877–1901, 2020. 1, 2, 9
- [6] Zhi Chen, Yijie Bei, and Cynthia Rudin. Concept whitening for interpretable image recognition. *Nat. Mach. Intell.*, 2(12):772–782, 2020. 9
- [7] Hyung Won Chung, Le Hou, Shayne Longpre, Barret Zoph, Yi Tay, William Fedus, Eric Li, Xuezhi Wang, Mostafa Dehghani, Siddhartha Brahma, et al. Scaling instruction-finetuned language models. *arXiv preprint arXiv:2210.11416*, 2022. 9
- [8] Mircea Cimpoi, Subhansu Maji, Iasonas Kokkinos, Sammy Mohamed, and Andrea Vedaldi. Describing textures in the wild. In *Proceedings of the IEEE conference on computer vision and pattern recognition*, pages 3606–3613, 2014. 1

- [9] Jia Deng, Wei Dong, Richard Socher, Li-Jia Li, Kai Li, and Li Fei-Fei. Imagenet: A large-scale hierarchical image database. In *CVPR*, pages 248–255. IEEE Computer Society, 2009. 4
- [10] Jacob Devlin, Ming-Wei Chang, Kenton Lee, and Kristina Toutanova. Bert: Pre-training of deep bidirectional transformers for language understanding. *arXiv preprint arXiv:1810.04805*, 2018. 9
- [11] Jack Dunn, Luca Mingardi, and Ying Daisy Zhuo. Comparing interpretability and explainability for feature selection. *CoRR*, abs/2105.05328, 2021. 8
- [12] Ali Farhadi, Ian Endres, Derek Hoiem, and David Forsyth. Describing objects by their attributes. In *2009 IEEE conference on computer vision and pattern recognition*, pages 1778–1785. IEEE, 2009. 1, 8
- [13] Riccardo Guidotti, Anna Monreale, Salvatore Ruggieri, Dino Pedreschi, Franco Turini, and Fosca Giannotti. Local rule-based explanations of black box decision systems. *CoRR*, abs/1805.10820, 2018. 8
- [14] Andrey Guzhov, Federico Raue, Jörn Hees, and Andreas Dengel. Audioclip: Extending clip to image, text and audio. In *ICASSP 2022-2022 IEEE International Conference on Acoustics, Speech and Signal Processing (ICASSP)*, pages 976–980. IEEE, 2022. 9
- [15] Kaiming He, Xinlei Chen, Saining Xie, Yanghao Li, Piotr Dollár, and Ross Girshick. Masked autoencoders are scalable vision learners. In *Proceedings of the IEEE/CVF Conference on Computer Vision and Pattern Recognition*, pages 16000–16009, 2022. 9
- [16] Jack Hessel, Ari Holtzman, Maxwell Forbes, Ronan Le Bras, and Yejin Choi. Clipscore: A reference-free evaluation metric for image captioning. *arXiv preprint arXiv:2104.08718*, 2021. 7
- [17] Chao Jia, Yinfei Yang, Ye Xia, Yi-Ting Chen, Zarana Parekh, Hieu Pham, Quoc V. Le, Yun-Hsuan Sung, Zhen Li, and Tom Duerig. Scaling up visual and vision-language representation learning with noisy text supervision. In *ICML*, volume 139 of *Proceedings of Machine Learning Research*, pages 4904–4916. PMLR, 2021. 9
- [18] Been Kim, Martin Wattenberg, Justin Gilmer, Carrie Cai, James Wexler, Fernanda Viegas, et al. Interpretability beyond feature attribution: Quantitative testing with concept activation vectors (tcav). In *International conference on machine learning*, pages 2668–2677. PMLR, 2018. 1
- [19] Been Kim, Martin Wattenberg, Justin Gilmer, Carrie J. Cai, James Wexler, Fernanda B. Viégas, and Rory Sayres. Interpretability beyond feature attribution: Quantitative testing with concept activation vectors (TCAV). In *ICML*, volume 80 of *Proceedings of Machine Learning Research*, pages 2673–2682. PMLR, 2018. 8
- [20] Diederik P Kingma and Jimmy Ba. Adam: A method for stochastic optimization. *arXiv preprint arXiv:1412.6980*, 2014. 4
- [21] Jan Kocoń, Igor Cichecki, Oliwier Kaszyca, Mateusz Kochanek, Dominika Szydło, Joanna Baran, Julita Bielaniewicz, Marcin Gruza, Arkadiusz Janz, Kamil Kanclerz, et al. Chatgpt: Jack of all trades, master of none. *arXiv preprint arXiv:2302.10724*, 2023. 1
- [22] Pang Wei Koh, Thao Nguyen, Yew Siang Tang, Stephen Mussmann, Emma Pierson, Been Kim, and Percy Liang. Concept bottleneck models. In *International Conference on Machine Learning*, pages 5338–5348. PMLR, 2020. 1, 4, 5, 8, 9
- [23] Jonathan Krause, Michael Stark, Jia Deng, and Li Fei-Fei. 3d object representations for fine-grained categorization. In *4th International IEEE Workshop on 3D Representation and Recognition (3dRR-13)*, Sydney, Australia, 2013. 4
- [24] Alex Krizhevsky, Geoffrey Hinton, et al. Learning multiple layers of features from tiny images. 2009. 4
- [25] Neeraj Kumar, Alexander C. Berg, Peter N. Belhumeur, and Shree K. Nayar. Attribute and simile classifiers for face verification. In *ICCV*, pages 365–372. IEEE Computer Society, 2009. 8
- [26] Christoph H. Lampert, Hannes Nickisch, and Stefan Harmeling. Learning to detect unseen object classes by between-class attribute transfer. In *CVPR*, pages 951–958. IEEE Computer Society, 2009. 8
- [27] Junnan Li, Dongxu Li, Caiming Xiong, and Steven Hoi. Blip: Bootstrapping language-image pre-training for unified vision-language understanding and generation. In *International Conference on Machine Learning*, pages 12888–12900. PMLR, 2022. 9
- [28] Adriano Lucieri, Muhammad Naseer Bajwa, Stephan Alexander Braun, Muhammad Imran Malik, Andreas Dengel, and Sheraz Ahmed. On interpretability of deep learning based skin lesion classifiers using concept activation vectors. In *IJCNN*, pages 1–10. IEEE, 2020. 8
- [29] Thomas McGrath, Andrei Kapishnikov, Nenad Tomasev, Adam Pearce, Demis Hassabis, Been Kim, Ulrich Paquet, and Vladimir Kramnik. Acquisition of chess knowledge in alphazero. *CoRR*, abs/2111.09259, 2021. 8
- [30] Sachit Menon and Carl Vondrick. Visual classification via description from large language models. *arXiv preprint arXiv:2210.07183*, 2022. 9
- [31] Maria-Elena Nilsback and Andrew Zisserman. Automated flower classification over a large number of classes. In *ICVGIP*, pages 722–729. IEEE Computer Society, 2008. 4
- [32] TB OpenAI. Chatgpt: Optimizing language models for dialogue. *OpenAI*, 2022. 1
- [33] Omkar M. Parkhi, Andrea Vedaldi, Andrew Zisserman, and C. V. Jawahar. Cats and dogs. In *CVPR*, pages 3498–3505. IEEE Computer Society, 2012. 4
- [34] P Jonathon Phillips, Carina A Hahn, Peter C Fontana, David A Broniatowski, and Mark A Przybocki. Four principles of explainable artificial intelligence. *Gaithersburg, Maryland*, 2020. 8
- [35] Sarah Pratt, Rosanne Liu, and Ali Farhadi. What does a platypus look like? generating customized prompts for zero-shot image classification. *arXiv preprint arXiv:2209.03320*, 2022. 9, 12
- [36] Alec Radford, Jong Wook Kim, Chris Hallacy, Aditya Ramesh, Gabriel Goh, Sandhini Agarwal, Girish Sastry, Amanda Askell, Pamela Mishkin, Jack Clark, et al. Learning transferable visual models from natural language supervision. In *International conference on machine learning*, pages 8748–8763. PMLR, 2021. 1, 9

- [37] Marco Túlio Ribeiro, Sameer Singh, and Carlos Guestrin. "why should I trust you?": Explaining the predictions of any classifier. In *KDD*, pages 1135–1144. ACM, 2016. 8
- [38] Marco Túlio Ribeiro, Sameer Singh, and Carlos Guestrin. Anchors: High-precision model-agnostic explanations. In *AAAI*, pages 1527–1535. AAAI Press, 2018. 8
- [39] Bernardino Romera-Paredes and Philip Torr. An embarrassingly simple approach to zero-shot learning. In *International conference on machine learning*, pages 2152–2161. PMLR, 2015. 1
- [40] Ramprasaath R Selvaraju, Michael Cogswell, Abhishek Das, Ramakrishna Vedantam, Devi Parikh, and Dhruv Batra. Grad-cam: Visual explanations from deep networks via gradient-based localization. In *Proceedings of the IEEE international conference on computer vision*, pages 618–626, 2017. 1
- [41] Ramprasaath R Selvaraju, Abhishek Das, Ramakrishna Vedantam, Michael Cogswell, Devi Parikh, and Dhruv Batra. Grad-cam: Why did you say that? *arXiv preprint arXiv:1611.07450*, 2016. 1
- [42] Hao Tan and Mohit Bansal. LXMERT: learning cross-modality encoder representations from transformers. In *EMNLP/IJCNLP (1)*, pages 5099–5110. Association for Computational Linguistics, 2019. 9
- [43] Aaron Van Den Oord, Oriol Vinyals, et al. Neural discrete representation learning. *Advances in neural information processing systems*, 30, 2017. 3
- [44] Catherine Wah, Steve Branson, Peter Welinder, Pietro Perona, and Serge Belongie. The caltech-ucsd birds-200-2011 dataset. 2011. 4, 5, 12
- [45] Zihan Wang, Chengyu Dong, and Jingbo Shang. "average" approximates" first principal component"? an empirical analysis on representations from neural language models. *arXiv preprint arXiv:2104.08673*, 2021. 5
- [46] Chen Wei, Haoqi Fan, Saining Xie, Chao-Yuan Wu, Alan Yuille, and Christoph Feichtenhofer. Masked feature prediction for self-supervised visual pre-training. In *Proceedings of the IEEE/CVF Conference on Computer Vision and Pattern Recognition*, pages 14668–14678, 2022. 9
- [47] Yujia Xie, Luowei Zhou, Xiyang Dai, Lu Yuan, Nguyen Bach, Ce Liu, and Michael Zeng. Visual clues: Bridging vision and language foundations for image paragraph captioning. *arXiv preprint arXiv:2206.01843*, 2022. 12
- [48] An Yan, Julian McAuley, Xing Lu, Jiang Du, Eric Y Chang, Amilcare Gentili, and Chun-Nan Hsu. Radbert: Adapting transformer-based language models to radiology. *Radiology: Artificial Intelligence*, 4(4):e210258, 2022. 9
- [49] An Yan, Xin Eric Wang, Tsu-Jui Fu, and William Yang Wang. L2c: Describing visual differences needs semantic understanding of individuals. *arXiv preprint arXiv:2102.01860*, 2021. 8
- [50] An Yan, Yali Wang, Zhifeng Li, and Yu Qiao. Pa3d: Pose-action 3d machine for video recognition. In *Proceedings of the IEEE/CVF conference on computer vision and pattern recognition*, pages 7922–7931, 2019. 8
- [51] Jianwei Yang, Chunyuan Li, Pengchuan Zhang, Bin Xiao, Ce Liu, Lu Yuan, and Jianfeng Gao. Unified contrastive learning in image-text-label space. *CoRR*, abs/2204.03610, 2022. 9
- [52] Yue Yang, Artemis Panagopoulou, Shenghao Zhou, Daniel Jin, Chris Callison-Burch, and Mark Yatskar. Language in a bottle: Language model guided concept bottlenecks for interpretable image classification. *arXiv preprint arXiv:2211.11158*, 2022. 1, 4, 5, 6, 9
- [53] Jiahui Yu, Zirui Wang, Vijay Vasudevan, Legg Yeung, Mojtaba Seyedhosseini, and Yonghui Wu. Coca: Contrastive captioners are image-text foundation models. *CoRR*, abs/2205.01917, 2022. 9
- [54] Lu Yuan, Dongdong Chen, Yi-Ling Chen, Noel Codella, Xiyang Dai, Jianfeng Gao, Houdong Hu, Xuedong Huang, Boxin Li, Chunyuan Li, Ce Liu, Mengchen Liu, Zicheng Liu, Yumao Lu, Yu Shi, Lijuan Wang, Jianfeng Wang, Bin Xiao, Zhen Xiao, Jianwei Yang, Michael Zeng, Luowei Zhou, and Pengchuan Zhang. Florence: A new foundation model for computer vision. *CoRR*, abs/2111.11432, 2021. 9
- [55] Mert Yükekönül, Maggie Wang, and James Zou. Post-hoc concept bottleneck models. *CoRR*, abs/2205.15480, 2022. 9
- [56] Tian Yun, Usha Bhalla, Ellie Pavlick, and Chen Sun. Do vision-language pretrained models learn primitive concepts? *arXiv preprint arXiv:2203.17271*, 2022. 1, 4, 5, 9
- [57] Susan Zhang, Stephen Roller, Naman Goyal, Mikel Artetxe, Moya Chen, Shuohui Chen, Christopher Dewan, Mona Diab, Xian Li, Xi Victoria Lin, et al. Opt: Open pre-trained transformer language models. *arXiv preprint arXiv:2205.01068*, 2022. 9
- [58] Jinghao Zhou, Chen Wei, Huiyu Wang, Wei Shen, Cihang Xie, Alan Yuille, and Tao Kong. ibot: Image bert pre-training with online tokenizer. *arXiv preprint arXiv:2111.07832*, 2021. 9

A. Prompt Design and Queried Attributes

A.1. GPT3

Inspired by recent work on querying LLMs [47, 35], we start with the following prompt and a demonstration to query GPT3:

Q: What are useful visual features to distinguish a lemur in a photo?

A: There are several useful visual features to tell there is a lemur in a photo:

- four-limbed primate
- black, grey, white, brown, or red-brown
- wet and hairless nose with curved nostrils
- long tail
- large eyes
- furry bodies
- clawed hands and feet

Q: What are useful visual features to distinguish *class_name* in a photo?

A: There are several useful visual features to distinguish *class_name* in a photo:

To elicit knowledge within a certain domain, we also test the following prompt to specify the domain given a task:

Q: What are useful visual features to distinguish *class_name* from other *domain_name* in a photo? A: There are several useful visual features to distinguish *class_name* from other *domain_name* in a photo:

Here *class_name* is the name of each class in the datasets. For instance, in CIFAR-10, *class_name* is from {airplane, automobile, bird, cat, deer, dog, frog, horse, ship, truck}. *domain_name* is the domain of the datasets. We set *domain_name* to be birds, objects, objects, flowers, foods, dogs and cats, cars, animals for datasets CUB, CIFAR-10, CIFAR-100, Flowwer, Food, Oxford-pets, Stanford-cars, Imagenet-Animals, respectively.

A.2. ChatGPT

Query ChatGPT for CUB As CUB is in a specific domain of bird species, we use ChatGPT to design structured and compositional attributes as in [44]. Specifically, we first query ChatGPT with the following prompts to obtain the possible names describing *body parts* for the birds:

What are the possible body parts to visually distinguish birds in the photo?

We obtain the following attributes for *body parts*:

$\mathcal{BP} = \{\text{wings, beak, feet, tail, head, breast, abdomen, leg, feathers}\}$.

Then we query for possible colors:

What are the possible colors that are possible to appear on a bird?

which results in a set of colors:

$\mathcal{C} = \{\text{red, orange, yellow, green, blue, purple, brown, black, white, gray}\}$.

Then we query the shapes of each possible body part, take wings for example:

What are the possible shapes for bird wings?

Finally, with the colors \mathcal{C} and the possible shapes for each body part shown in Table 7, we build 440 attributes for CUB with examples shown below:

red swallowtail or fork-tailed wings.
red round wings.
green webbed legs.
orange round wings.

Query ChatGPT for CIFAR-100 We utilize the batch prompting method described in Section 2 to query ChatGPT for the attributes of CIFAR-100.

We use the following prompt to query ChatGPT:

Q: Here are five *superclass_name*: {*class_name_1*, ..., *class_name_N*}. What are the useful visual features for distinguishing them in a photo? Please list every attribute in bullet points.

Here *superclass_name* is the name of each superclass in the datasets. For instance, in CIFAR-100, beaver, dolphin, otter, seal, whale belongs to the superclass aquatic mammals.

A.3. Comparing Different Attribute Concept Pools

With the above prompting templates, we explore the effects of different concept pools. Comparing with the concept pool constructed from GPT-3 prompts with corresponding class names for each dataset, we add the following two pools to discuss the effects: (1) the concepts from Imagenet queried from GPT-3, which would be larger and also noisier; (2) The concepts from ChatGPT. Note that we conduct the ablation study on two dataset CUB and CIFAR-100, since their classes are generally covered by the classes from Imagenet. For CUB, we manually designed the attributes in the pool and for CIFAR-100, the attributes are

Body parts	Possible shapes
wings	Swallowtail or fork-tailed wings, Round wings, Long, narrow wings, Short, broad wings, Elliptical wings
beak	Conical beaks, Hooked beaks, Probe-like beaks, Wide, flat beaks, Short, stubby beaks, Long, thin beaks
feet	Webbed feet, Talons, Perching feet, Scaling feet, Running feet
tail	Fan-shaped tails, Square-shaped tails, Rounded tails, Forked tails, Tails with streamers
head	Conical heads, Round heads, Elongated heads, Wide heads, Stout heads, Narrow heads
breast	Flat breasts, Round breasts, Bulky breasts, Slender breasts
leg	Long and slender legs, Short and thick legs, Webbed legs, Talons legs, Perching legs
abdomen	Round and plump abdomen, Slim and streamlined abdomen, Long and thin abdomen, Puffed out abdomen
feathers	Long, narrow feathers, Short, broad feathers, Round feathers, Streamer-like feathers

Table 7: Possible shapes for each body part of birds.

queried in a hierarchical way (see Appendix A for the details). The results are shown in Table 8.

Overall, our learning-to-search method is robust to different attribute pools, and we do not observe significant performance change using GPT-3 or ChatGPT. Though our human-designed compositional attributes with ChatGPT on CUB is worse than pure LLM-generated attributes.

Datasets	CUB			CIFAR-100		
K	8	16	32	8	16	32
GPT-3	31.67	48.55	60.27	34.77	52.24	66.30
GPT-3-Imagenet	30.81	49.29	60.41	33.80	51.01	65.61
ChatGPT	21.66	40.28	47.46	33.79	51.26	67.06

Table 8: Comparison *w.r.t.* different Concept Pools.

A.4. Robustness Check

To confirm the effectiveness of our prompts and the robustness of GPT-3 prompts, we conduct the experiments with the concepts queried from GPT3 using different prompts. We design semantically instructive and misleading prompts as shown in Table 9. Overall, we observe that other instructive prompts perform similar to ours, while misleading prompts could hurt the performance drastically.

B. Implementation Details

B.1. Linear Probing

After we obtain attribute embeddings \mathbf{T}^* from Eq.(6), we then calculate the semantic vector \mathbf{A}^* of each image I with the D -dimensional image embedding $\mathbf{V} = \Theta_V(I) \in \mathbb{R}^D$:

$$s_j = \cos(\mathbf{V}, \mathbf{T}_j^*), j = 1, \dots, K, \quad (8)$$

$$\mathbf{A}^* = (s_1, \dots, s_K)^\top. \quad (9)$$

Then we calculate the score vectors of all the images in the training and testing dataset. We then use linear probing to evaluate the performance. Since we use a task-guided searching during the first stage to find K attribute embeddings, we can readily use the classification head in the first stage (i.e., a linear model $f_\theta \in \mathbb{R}^K \rightarrow \mathbb{R}^{K_C}$ with one fully connected layer) for our second stage with lightweight fine-tuning instead of training from scratch. where K_C is the number of classes. Then, we train f_θ with a cross-entropy loss:

$$\mathcal{L} = -\frac{1}{M} \sum_{i=1}^M \sum_{c=1}^{K_C} y_{i,c} \log p'_{i,c}, \quad (10)$$

the same as Eq.(2), M is the number of images in a mini-batch. $y_{i,c}$ is the binary indicator of i -th image the mini-batch belonging to class c , and $p_{i,c}$ is the predicted probability of the i -th image belonging to class c . Then $p'_{i,c}, c \in \{1, \dots, K_C\}$ is calculated as:

$$[p'_{i,1}, \dots, p'_{i,K_C}]^\top = \text{Softmax}(f_\theta(\mathbf{A}_i^*)) \quad (11)$$

where \mathbf{A}_i^* is the semantic vector of the i -th image in the mini-batch. Then we will use f_θ to classify the images in the test set to yield the performances.

Category	Prompts	Acc
Instructive	What are the useful visual features to distinguish <i>class_name</i> ?	31.67
	What are the helpful visual features to distinguish <i>class_name</i> ?	32.71
	What are the distinctive visual features to distinguish <i>class_name</i> ?	30.38
Misleading	What are the useless visual features to distinguish <i>class_name</i> ?	19.64
	Give me some random visual features in a photo to distinguish <i>domain_name</i> :	5.85

Table 9: Robustness study against different prompts on CUB, with $K = 8$

C. Additional Experiments

C.1. Comparison with Zero-Shot Classifications

Datasets	CIFAR-100	Stanford-cars
CLIP-ZS w/ class names	54.49	57.87
CLIP-ZS w/ attributes	30.07	5.42
CLIP-Train Visual	79.30	79.95
Ours (K=512)	75.41	74.67
Datasets	Flower	Imagenet-Animals
CLIP-ZS w/ class names	60.19	59.44
CLIP-ZS w/ attributes	9.80	9.13
CLIP-Train Visual	92.35	75.31
Ours (K=512)	90.29	75.60

Table 10: Comparison with zero-shot classification methods.

We deliver more results in Table 10. We use *A photo of* as the prompt for all methods. Zero-shot (CLIP-ZS) is worse than supervised training. Note that CLIP-ZS with class names may not be a fair comparison, **as our goal is to classify images with attributes instead of class names**, thereby gaining a level of interpretability and fine-grained understanding of visual recognition. If we use only attributes for CLIP-ZS, the performance drastically decreases.

C.2. Human Evaluation

To further evaluate the quality of our learned attributes, we conduct a pairwise human evaluation on Amazon Mechanical Turk. Specifically, we compare our attributes with uniformly sampled attributes from the GPT-3 generated attributes, and ask human to decide which set of attributes are better. Since datasets with hundreds of classes are hard to reason and compare, we evaluate our results on CIFAR-10. We sample 100 sets of 4 attributes from the attribute pool, and create 100 pairs of each random set of 4 attributes with our learned 4 attributes. Each pair was assigned to 5 workers to eliminate human variance. For each attribute pair, workers are presented with sampled images from CIFAR-

Choice (%)	Ours	Uniform	Tie
Score	31.6	19.0	49.4

Table 11: Human evaluation results on CIFAR-10. Human are asked to vote which attributes are better, where *tie* means the two sets looks the same to annotators

Model Architectures	8	16	32
CLIP RN50	24.28	38.95	56.11
CLIP RN101	27.36	46.10	56.06
CLIP RN50x16	28.91	53.46	57.69
CLIP ViT-B/32	31.67	48.55	60.27
CLIP ViT-B/16	36.69	55.64	63.70
CLIP ViT-L/14	38.71	65.52	74.99
CLIP ViT-L/14@336px	40.95	66.58	76.04
Open-CLIP ViT-H-14 LAION-2B	49.84	73.28	82.60

Table 12: Ablation study on different VLMs with bottleneck size $K=8,16,32$ on the CUB dataset.

10. We instruct the workers to consider which set of attributes are more useful to classify the 10 classes. As shown in Table 11, even though in most cases, the attributes look similar to human, workers still favor *Our method* over *Uniform sampling*, which is consistent with the classification accuracy.

D. More ablations

Better V&L models We evaluate different variants of CLIP style models, as shown in Table 12. Overall, our method is model-agnostic. It can be applied with any VLMs that compute image-text similarities. We also observe that in general, a stronger VLM will result in more accurate estimation of semantic vectors, hence improves classification performance.

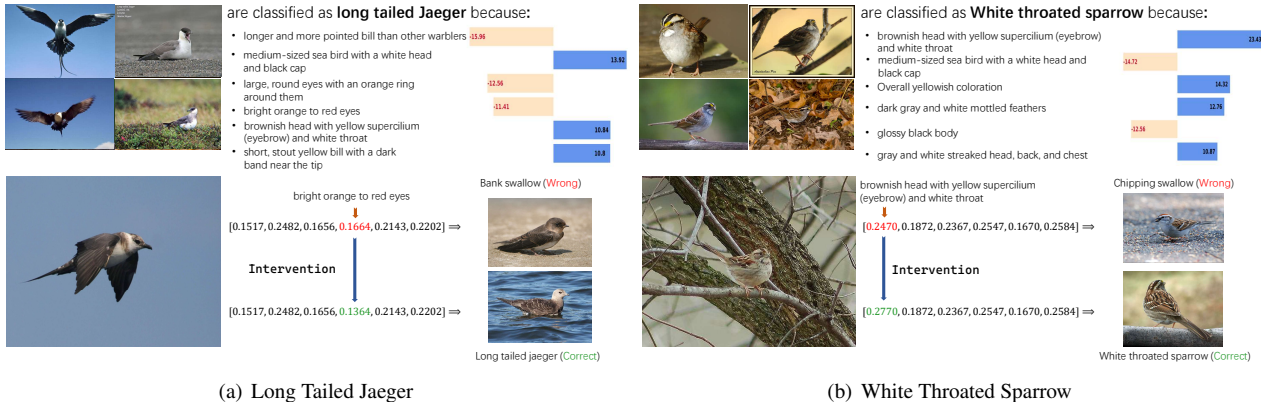


Figure 8: Examples on interpretability and interactivity. (1) The upper half of each figure show important attributes for two classes of birds. We choose 6 out of 32 attributes with highest importance scores, which are computed by multiplication between clip scores and weights in the linear probe, defined in Eq. (7). (2) The lower half of each figure demonstrates the intervention on the semantic vector (i.e., CLIP scores) to correct the prediction, we use $\delta=0.03$ for all interventions on clip scores as an empirical value. The array of 6 scores are of the same order as the attributes.

Datasets	CUB			CIFAR-100		
	8	16	32	8	16	32
One-Hot	36.22	44.35	48.96	57.90	61.85	65.43
Only Top Scores	36.03	44.32	49.43	58.32	61.90	65.86

Table 13: Comparison between scores and one-hot

Effectiveness of semantic projection. Scores vs one-hot

In this part, we consider the following baseline to show that the information within the similarity scores are useful: For an image I , after calculating all the similarity scores between every attribute $a_i \in \{a_1, \dots, a_N\}$ and the image I to obtain the vector $\mathbf{A} \in \mathbb{R}^N$. Then we wipe out the information in the scores by setting top- K large scores in \mathbf{A} as 1, and setting the left scores as 0, which will give us a binary vector $\mathbf{A}_{bin} \in \{0, 1\}^N$. Then we train and test the classification model on the corresponding binary vectors to compare with our methods. We conduct the ablation study on CUB as an example. We choose $K = 8$ and $K = 16$ for the comparisons.

From the results in Table 13, we observe the information from the similarity scores provides information for classification, while removing the information in the scores (converting top-K scores to 1) may lead to performance drop.

GPT-3 attributes vs. Random words We present more results on 8 datasets to verify that a large number of GPT-3 attributes behaves similar as random words. The observations are coherent on all eight datasets. When K is large, even if we randomly create K meaningless phrases from the entire vocabulary, we can still obtain competitive classification performance.

	Nonsense		GPT3	
	4	512	4	512
K				
CUB	2.42	64.79	12.98	67.64
CIFAR-10	31.26	92.81	60.30	93.67
CIFAR-100	10.17	77.40	16.13	77.55
Flower	3.33	90.20*	28.92	90.78*
Food	7.79	82.65*	16.23	82.50*
Oxford_pets	14.31	83.61*	28.07	86.01*
Stanford_cars	5.06	75.09	13.41	75.13
Imagenet_Animals	3.78	75.12	8.81	75.75

Table 14: GPT3 vs Nonsense. * means the results are obtained when setting the number of attributes to the size of the concept pool from GPT3, which corresponding to the results of "full" in Figure 4.

E. Additional Case Study

E.1. Test-time Intervention

We provide more case studies in Figure 8 to show the interpretability and interactivity of our method.

E.2. Visualization of Discovered Attributes

We present our learned 32 attributes for each dataset (by setting $K = 32$) in Table 15 and 16. Similar to Figure 6, we can observe these attributes are distinctive within each domain, and provides fine-grained attributes to summarize a dataset. To some level, we can view these automatically learned attributes as a form of knowledge to help humans understand how visual recognition works.

Dataset	Learned 32 attributes for each dataset
CUB	(1) Brown, gray and white feathers on the upper parts of the body, with a rusty red or pinkish tinge to the head; (2) bright yellow and black coloring; (3) distinctive white throat; (4) Broad tail that is shorter than other pelican species ; (5) short legs for perching in trees ; (6) bright yellow throat, breast, and flanks with black bars ; (7) Brown and white mottled back ; (8) pinkish red breast patch with white edges ; (9) white throat patch bordered by black stripes ; (10) unique pattern of spots on lower throat and breast.; (11) Large feet for scratching in leaf litter; (12) brownish head with yellow supercilium (eyebrow) and white throat ; (13) red or orange coloration; (14) iridescent black body with blue and purple highlights ; (15) red, black and white feathers; (16) grayish brown body with darker wings and tail; (17) Heavy bill for crushing seeds ; (18) olive green back and wings; (19) white throat, belly and wing bars ; (20) Long, slender bill with yellow tip; (21) large, white bird; (22) grayish brown head and back; (23) red/orange coloration on the face during breeding season; (24) Gray head and yellow throat with white eye rings; (25) barred wings and tail feathers in black, white and grey patterning ; (26) distinctive white throat patch ; (27) long, heavy bill; (28) yellow head; (29) male mallards have a green head, yellow beak and white neck ring; (30) Broad white eyering ; (31) white throat and belly region; (32) bright orange and black plumage
CIFAR-10	(1) antlers (in males); (2) some birds have crests on their heads; (3) propellers or jet engines; (4) fur coat of varying colors and patterns; (5) a tail with a horizontal stabilizer; (6) portholes along the hull; (7) large body with a cab and a bed; (8) landing gear; (9) four wheels; (10) fuselage and other structural elements; (11) four-wheeled vehicle; (12) long head with a mane and tail; (13) has a mast with sails or flags; (14) paws with clawed toes; (15) feathers of various colors and patterns; (16) tail lights; (17) furry body; (18) a beak or bill for eating, preening, and other activities; (19) pointed bow and stern; (20) mane of hair along the neck and back; (21) masts, sails, and rigging; (22) two wings and two legs; (23) moist slimy skin; (24) windshield and side windows; (25) rudders at the stern for steering; (26) smokestacks or funnels on top of the ship; (27) a large deck or superstructure; (28) hooves on each foot; (29) typically has a steering wheel and pedals for driving; (30) control surfaces (flaps, ailerons, rudder); (31) grille or front fascia; (32) may have a cargo area in the back
CIFAR-100	(1) A pair of pedipalps near the mouth used for sensing, holding prey and mating; (2) multiple petals in shades of pink, red, yellow or white; (3) Headboard and footboard; (4) pouch on the abdomen of female kangaroos; (5) fruits are two winged samaras in clusters; (6) large courtyard area surrounded by buildings; (7) orange or yellow fur with black stripes; (8) buds clustered at branch tips in winter months; (9) large wheels and tires; (10) Mattress and bedding; (11) large, floppy ears; (12) silver scales with black and red spots on the sides; (13) long snout with sharp teeth; (14) smooth oval shaped sepals; (15) clustered, coconuts at the tip of each branch; (16) white foam from waves breaking against rocks and shorelines; (17) designs, colors, or patterns on the can; (18) shaggy fur; (19) tailgate at rear end; (20) long bushy tail usually with a tuft of hair at the end; (21) portcullis at entrance to gatehouse; (22) cabin or operator’s seat in the middle of the vehicle; (23) drawbridge over a moat; (24) dialing pad with numbers 0–9; (25) catkins (flowers) in spring; (26) a large, tawnycolored body with a shaggy mane; (27) Ten walking legs and two large antennae; (28) Rim around the edge of the bowl; (29) armrests and backrests; (30) Long stem or pole extending from the shade to the base; (31) an ovary located at the base of the flower; (32) waxy texture of the petals and leaves
Flower	(1) bright purple petals that are fused together to form a thistle-like shape; (2) trumpet shaped flowers in shades of blue, purple, and white; (3) blue, purple, or white flowers with a thistle-like appearance; (4) an upright inflorescence (flower spike) bearing several clustered flowers on each branch ; (5) umbel of several small flowers on top of a single stem ; (6) Center of the spathe that looks like a tail or spadix; (7) the flower is a daisy-like plant with white petals and yellow center; (8) layered petals with a yellow center and pink edges ; (9) Large, bright pink to red flower ; (10) Six distinct petal segments surrounding an inner cup of short filaments and a trumpet center.; (11) trumpet shaped orange center with yellow stamens protruding from it ; (12) large, white petals with a yellow center; (13) fragrant single or double blooms in white, pink, or red; (14) brightly colored petals in shades of oranges, reds, and yellows; (15) large, yellow petals that form a daisy-like shape; (16) umbrella shaped clusters of white to pinkish flowers ; (17) tall, leafless stem; (18) hibiscus shaped leaves that are serrated around the edges; (19) pink to purple colored petals with red lips; (20) single stem with a rosette of leaves; (21) tall, slender stem with a single umbel of flowers; (22) large blue or purple flowers with five petals and a hooded center; (23) intricate patterns of blue, purple, pink and white lines on the petals ; (24) yellowish green sepals below the flower; (25) dark purple petals; (26) five petals arranged around a central column of white stamens and stigma ; (27) pink, white, or lavender flowers with five petals; (28) bright yellow flower head; (29) bright pink, red, or white petals with fringed edges; (30) bright red, orange, or yellow blooms; (31) bright red and yellow petals; (32) deep red, orange or yellow petals

Table 15: Learned 32 attributes on CUB, CIFAR-10, CIFAR-100 and Flower.

Dataset	Learned 32 attributes for each dataset
FOOD	(1) sliced strawberries arranged over the cream/whipped topping; (2) A white or wheat bun with a golden brown exterior ; (3) Long, thin rice noodles; (4) lattice pattern on the top layer made by weaving strips of pastry dough; (5) slices of apples arranged in a spiral pattern ; (6) large pieces of clams visible in the chowder; (7) Gyoza is typically shaped like a half-moon or dumpling and can have either open or closed tops. ; (8) The broth will usually have either a sour or spicy taste depending on the type of soup ; (9) red sauce layered between the noodles and cheese; (10) shredded carrots embedded within the cake ; (11) dollop of sour cream or guacamole ; (12) thin layers of phyllo dough; (13) tender squid rings inside ; (14) distinctive pattern of takoyaki sauce on top; (15) moist and dark brown cake with visible cocoa powder; (16) Served on top of a bed of shredded daikon radish or grated daikon ; (17) lobster chunks mixed with mayonnaise and spices; (18) two layers of toast with lettuce, bacon, and tomatoes in between; (19) mashed avocado texture ; (20) cooked shrimp in a variety of colors (pink, orange, etc.); (21) steaming bowl of soup with steam rising up ; (22) melted cheese over the chips; (23) The presence of Mandarin pancakes, cucumber slices and spring onion used in traditional preparation methods; (24) fried or served cold with dipping sauce; (25) a custard base topped with a layer of hardened caramelized sugar; (26) a dollop of gochujang (red pepper) paste ; (27) butter or oil is used to toast the bread on both sides ; (28) chunks of vegetables, tofu, and seaweed floating in it; (29) gooey mixture of sugar, butter and cinnamon visible between the layers of apple slices; (30) olive oil and soy sauce dressing ; (31) toppings such as egg, vegetables, seaweed, and pork slices ; (32) toppings such as jalapenos, tomatoes, onions and/or peppers
Oxford-pets	(1) Long legs and neck; (2) large upright ears; (3) “Ragdoll” appearance with a long body and short legs; (4) Soft wiry coat in black or brindle colors; (5) Pointed ears; (6) Shade of red or wheaten color; (7) dark brown or black coat with white markings; (8) Markings resembling a leopard or tiger in various colors (brown, black, white, orange); (9) mediumsized dog; (10) greyish blue fur with silver tips; (11) short, almost hairless body with wrinkles; (12) Round eyes in shades of blue or green; (13) White and grey fur; (14) A tail that curls over its back; (15) Ears that are small and rounded at the tips; (16) loose skin on the face and neck that can create wrinkles; (17) triangular ears; (18) white blaze on face and chest; (19) droopy ears that hang close to the head; (20) wide eyes with prominent wrinkles around them; (21) thick, white double coat; (22) foxy head and face with a curled tail; (23) Curly tail that curls over the back; (24) black face mask on white fur background; (25) long, silky coat in white or white and black colors; (26) thick mane around neck and chest; (27) distinctive wrinkles on the face; (28) short coat of glossy black fur; (29) Short, glossy coat of black and silver; (30) double coat of fur that is typically fawn, black or silver; (31) black and tan coloring; (32) Visible spots on the body
Stanford-cars	(1) large grille with a classic Bentley badge; (2) Signature wheel arches; (3) large tailgate spoiler on the liftgate; (4) unique wheels with five spokes and silver finish; (5) Front bumper has a skid plate design; (6) flared wheel arches that give the car an aggressive look; (7) Ron Fellows Edition badge on the rear of the car; (8) The distinct hexagonal grille with the Volvo emblem at the center; (9) Distinctive red and black racing stripes with Abarth logo; (10) “4Runner” badge on the rear liftgate; (11) Hatchback style trunk/boot area; (12) High performance tires with “Type R” on the sidewall; (13) horizontal three bar tail lamps with the running Mustang logo at its center.; (14) distinctive grille with a mesh pattern and Spyker logo; (15) Interior: Leather wrapped steering wheel with audio controls; (16) kidney grille with large blue and white BMW logo; (17) black power convertible top; (18) Red badge with “Integra Type R” logo or lettering on the hood and trunk lid; (19) Chrome grille with the Chevrolet logo; (20) the Fiat logo on the front grille and rear of car; (21) Quattro badge on the rear right side of the car; (22) gloss black paint job with distinct yellow detailing; (23) LED tail lights with a unique curved design to give it a modern look.; (24) Chrome grille with the Chrysler emblem in the center; (25) chrome grille with the Chevrolet logo; (26) wide grille with a large chrome Bentley badge in the center; (27) two door hardtop convertible body style; (28) distinctive side windows with curved lines and signature Maybach logo; (29) tailgate spoiler on the rear hatchback door; (30) Chrome grille outlining the Honda logo; (31) Black brake calipers with Corvette lettering; (32) Twodoor, fourseater convertible hardtop
Imagenet-Animals	(1) smaller and lighter than other Welsh corgis; (2) from Airedale, England; (3) male rams have large, thick horns, while female rams have smaller, thinner horns; (4) dense, flat coat; (5) the Maltese has a reputation for being lively, playful and affectionate; (6) coat is predominantly black and tan; (7) Gordon setters are typically black with tan markings; (8) Saint Bernards are large dogs; (9) Kerry blue terriers are from Ireland; (10) the breed name (elkhound); (11) English setters are bred in England; (12) shaggy, matted coat; (13) all black coat; (14) spotted or striped fur; (15) dark brown or black coat with a distinctive “water spaniel” curl; (16) glossy black feathers with a green or blue sheen; (17) pink, orange, or yellow stripes on the shell; (18) black and white, blue and white, or wheaten (red) coloration; (19) wrinkles on the face and head; (20) coat is wheaten in color (ranging from pale cream to rich gold); (21) big ears; (22) male finches have a bright red breast; (23) creamy white or wheaten-colored coat; (24) white throat; (25) large, broad carapace; (26) dark plumage with black and iridescent blue feathers; (27) long, black antennae; (28) large, black and white dolphin; (29) longer legs than other hound breeds; (30) fawn or brindle coloration; (31) long, wirehaired coat; (32) fawn to mahogany coat

Table 16: Learned 32 attributes on Food, Oxford-pets, Stanford-cars and Imagenet-Animals.